Vol. 692: 81–97, 2022
https://doi.org/10.3354/meps14079

MARINE ECOLOGY PROGRESS SERIES
Mar Ecol Prog Ser

Published June 30

Dietary shifts and niche partitioning throughout ontogeny reduce intraspecific competition in a pelagic generalist predator

Xiaodi Gao[1,2], Yi Gong[1,2,3,4,5], Xinjun Chen[1,3,4,5], Yunkai Li[1,2,3,4,5,*]

[1]College of Marine Sciences, Shanghai Ocean University, Shanghai 201306, PR China
[2]Laboratory for Marine Fisheries Science and Food Production Processes, Qingdao National Laboratory for Marine Science and Technology, Qingdao 266071, PR China
[3]Key Laboratory of Oceanic Fisheries Exploration, Ministry of Agriculture and Rural Affairs, Shanghai 201306, PR China
[4]National Engineering Research Center for Oceanic Fisheries, Shanghai Ocean University, Shanghai 201306, PR China
[5]Key Laboratory of Sustainable Exploitation of Oceanic Fisheries Resources, Shanghai Ocean University, Ministry of Education, Shanghai 201306, PR China

ABSTRACT: Patterns of feeding strategy change throughout ontogeny according to size-specific abilities and requirements. Characterizing the extent and potential repeated occurrence of dietary differences within the population can improve understanding of the intraspecific predation regime and population dynamics. Here, we investigated size-related feeding habits and trophic niche partitioning of an iconic pelagic generalist predator, the jumbo squid *Dosidicus gigas*, by a combined analysis of morphologic indicators of feeding capability (fin and feeding apparatuses), trophic biochemical tracers (stable isotopes and fatty acids), and stomach contents. Results showed significant variation in prey composition, isotopic values, and fatty acid profiles with size. *D. gigas* exhibited a shift in diet at approximately 250 mm mantle length (ML). The trophic niche of small (ML ≤ 250 mm) and large (ML > 250 mm) squid revealed low potential for resource overlap, suggesting segregation in terms of spatial and food resources of different size groups. Large individuals tend to feed deeper and on smaller prey to optimize food capture costs and energy benefits. This feeding strategy is likely related to variability in the development of feeding capacity, increasing swimming ability, and metabolic demand as squid grow and may reduce intraspecific competition to improve survival. These results highlight the dietary flexibility of *D. gigas* and demonstrate that niche differentiation acts as a major factor in a cohort, which may have important implications for their population dynamics and management. In addition, this study demonstrates that using multiple diet tracers can highlight subtle differentiations in diet correlated to growth in a pelagic generalist predator.

KEY WORDS: *Dosidicus gigas* · Feeding apparatus · Stomach content · Stable isotope · Fatty acid · Trophic niche

1. INTRODUCTION

The occurrence of ontogenetic, or size-related, shifts in diet or habitat is prevalent and important in shaping species interactions and structuring communities (Werner & Gilliam 1984). The Ommastrephidae have diversified morphology, growth patterns, and lifestyles from paralarvae to adults (Fernández-Álvarez et al. 2018). Bigger individuals have 2 longer unique independent raptorial tentacles, harder and sharper beaks, stronger arms and nervous and sensory systems, and bigger fins, allowing the squid to cover greater predation distances, prey on larger and more energetic prey, and swim faster than small conspecifics (Kier & Smith 1985, Shigeno et al. 2001, Shea 2005, Nödl et al. 2016, Fernández-Álvarez et al.

*Corresponding author: ykli@shou.edu.cn

2017, 2018). Morphological development of Ommastrephidae coincides with dietary shifts from small crustaceans to larger fish species and cephalopods, indicating that the size and morphology of the capture apparatus may reflect the capacity to seize or bite for prey, which is assumed to be the result of adaptations to different feeding spectra, and resulting in the flexible trophic niche of squid during ontogeny (Franco-Santos & Vidal 2014, Gong et al. 2018b, Trasviña-Carrillo et al. 2018). Collectively, these attributes allow squid of a certain size to expand their trophic niche.

The jumbo squid *Dosidicus gigas* is the most abundant ommastrephid squid in the eastern Pacific, with a wide distribution, from California (37° N) to southern Chile (47° S) and in waters from the neritic to the mesopelagic zones (depths up to 1200 m). This species supports the world's largest cephalopod fishery, with a commercial average catch of ~1 million t yr^{-1} in the 5 yr period from 2014 through 2018 (FAO). Its high productivity makes this species a profitable fishery, which is important to human populations, especially in coastal areas such as Peru and Mexico. Since 2004, China has become the second-largest *D. gigas* fishery in the Southeast Pacific Ocean (FAO). However, little is known about jumbo squid population dynamics; thus there is an urgent need to increase our knowledge in this field.

Examining the food and feeding habits of an abundant species is important for evaluating the ecological role and its position in the food web of ecosystems. Feeding is assumed to be the key factor in controlling population growth, reproduction, mortality, and migration patterns, which are considered relevant data for fishery management (Nesis 1970, Lorrain et al. 2011, Argüelles et al. 2012). *D. gigas* is recognized as playing a critical role in the pelagic ecosystem as both prey and predator, acting as a trophic link and transferring nutrients and energy from micronekton to large top predators (Friedemann et al. 2008, Argüelles et al. 2012, Trasviña-Carrillo et al. 2018). The species is short-lived, with a life span of 1 to 2 yr (Nigmatullin et al. 2001). Being an active predator with a high growth rate, it requires large amounts of energy to meet its metabolic and physiological needs and follow or search for food during the day and night (Gilly et al. 2006, Rosa & Seibel 2010, Rosas-Luis et al. 2011).

Studies have found that *D. gigas* shows highly opportunistic feeding behavior that includes cannibalism. Variations in the composition of the diet are related to predator size, prey availability, and environmental variability (Lorrain et al. 2011, Field et al. 2013). The prey spectrum of *D. gigas* changes during ontogeny from crustaceans to nektonic fishes and squids (Shetinnikov 1989). It seems that larger squid can consume larger prey items, reflecting different foraging strategies (Ruiz-Cooley et al. 2006, Argüelles et al. 2012, Field et al. 2013). However, identifying the key point at which that dietary shift or trophic niche divergence occurs during their growth is difficult. The use of available resources during ontogenetic development can be a key strategy for the survival of a species with a large abundance in the eastern Pacific. Thus, characterizing the extent and repeatability of dietary differences among different sizes can improve our understanding of the intraspecific predation regime of *D. gigas* and their population dynamics.

Stomach content analysis (SCA) of hard parts that are resistant to digestion (e.g. squid beaks, fish otoliths, and crustacean exoskeletons) allows prey identification at different taxonomic levels, which can provide recent and detailed information about what animals eat (Hyslop 1980). Yet, a limitation of the visual inspection of squid stomach contents is that the prey items are often beyond recognition due to maceration or digestive erosion (Rodhouse & Nigmatullin 1996). DNA sequencing of stomach contents can provide further insight into prey species composition (Frézal & Leblois 2008, Field et al. 2013). Since the prey items of squids are known to be bitten into small pieces before being swallowed, rapidly digested, and rejected, SCA alone may have a certain randomness and may be hampered when identifying prey items, especially for cephalopods (Argüelles et al. 2012). Furthermore, stomach contents represent only the last feeding event (<24 h) and therefore do not provide sufficient information about the average trophic position and food sources.

Stable isotope analysis (SIA) and fatty acid analysis (FAA) are the 2 natural chemical tracers that can reflect time-integrated information on food assimilated in tissues over timescales of weeks and years (Iverson et al. 2004, Baeta 2019). Carbon stable isotope ratios ($\delta^{13}C$) change slightly (0–1‰) from diets to consumers, allowing the identification of the sources of primary productivity; nitrogen stable isotope ratios ($\delta^{15}N$) show a more amplified enrichment (2.5–3.4‰) through trophic transfer, and the relative trophic level and breadth can be inferred (Post 2002). Fatty acids (FAs) are lipid constituents that are important to physiological and biochemical processes. Essential FAs are unable to be synthesized by all consumers, fully depending on dietary sources. They are considered to originate from marine phyto-

plankton (autotrophic) and symbiotic microorganisms (heterotrophic) and are then transferred conservatively to consumers, as n-3 and n-6 long-chain polyunsaturated FAs (PUFAs) (Volkman et al. 1989, Bell et al. 1994, Drazen et al. 2009). Thus, the FAs of individuals can provide a wide range of dietary information. FAs derived from storage lipids provide energy for growth, reproduction, and survival, varying with the physiological status of organisms, especially the reproductive status, which can provide far more detailed dietary information than SCA and SIA (Narváez et al. 2008). Combining SIA and FAA allows the estimation of the intra- or interspecies relationships of trophic niches and provides deeper insights into resource partitioning and energy allocation, reducing the bias produced from prey with a random appearance in SCA (Sardenne et al. 2016).

Previous studies reported a relationship between morphological development and dietary selection (Franco-Santos & Vidal 2014, Fernández-Álvarez et al. 2018). The use of food in animals is associated with anatomical differences in the structures required to find and process food. The morphological structure of feeding apparatuses can be thought of as a functional adaption resulting from the type of food intake (Skieresz-Szewczyk & Jackowiak 2016, Gong et al. 2020). Combining morphometric analysis with feeding ecology has been proved to be a complementary method for describing the spatial patterns of feeding and habitat use (Gong et al. 2020).

In this study, we combined 20 morphometric variables of feeding apparatuses and a multiple-technique approach (SCA, SIA, and FAA) to investigate patterns in dietary shift and trophic plasticity under ontogenetic influences. Our aims were to (1) explore whether there is a shift in diet and the possible occurrence periods throughout ontogeny and (2) examine the extent of resource partitioning, trophic interaction, and foraging strategies with ontogeny for *D. gigas* within the equatorial Pacific Ocean. We hypothesized that *D. gigas* partitions the food resources associated with its growth to reduce intraspecies competition.

2. MATERIALS AND METHODS

2.1. Sample collection

Jumbo squid specimens were collected randomly at night by hand jigging during June and July 2017 (Fig. 1). All samples were immediately stored onboard and kept frozen (–30°C) and were then transferred to the laboratory for processing. For each specimen, the dorsal mantle length (ML), fin length (FL), and fin width (FW) were measured to the nearest mm and weighed to the nearest gram after defrosting. Sampled squids were then dissected to determine sex and gonad maturity stage based on the 5-stage scale from Arkhipkin & Laptikhovsky (1994): stages I and II (immature), III (maturing), and

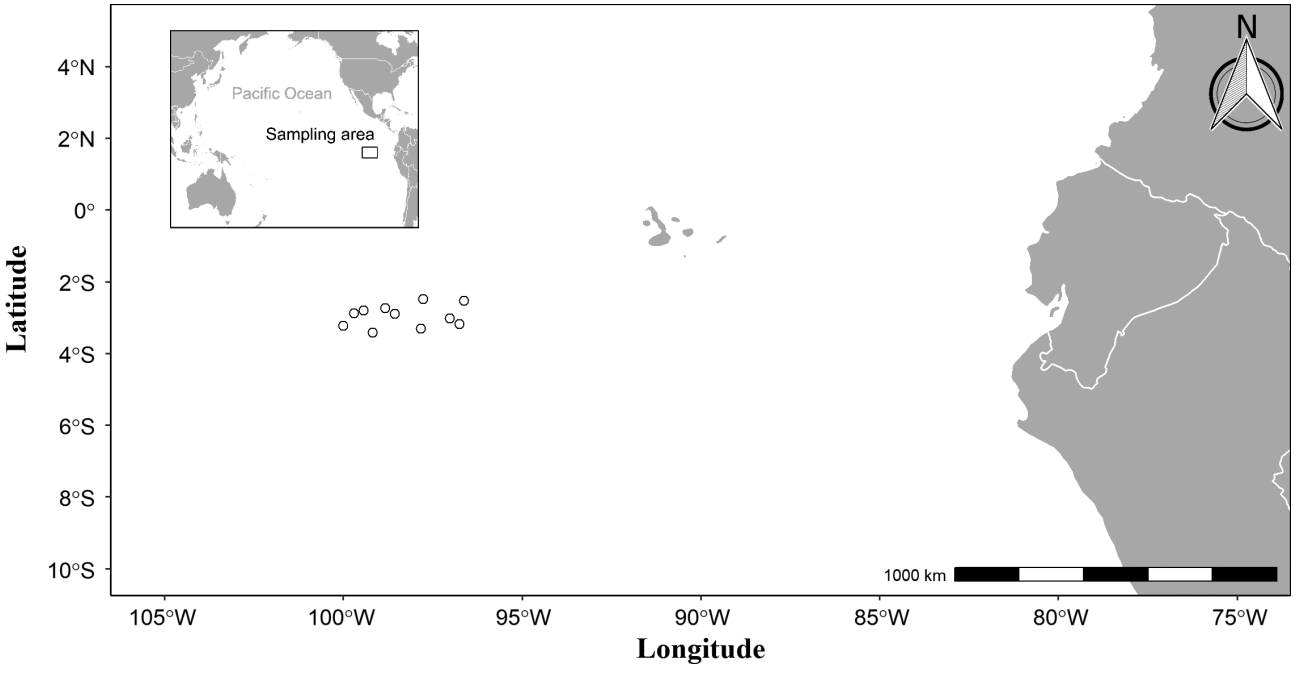

Fig. 1. Sampling locations in the eastern equatorial Pacific Ocean

Table 1. Number of individuals of *Dosidicus gigas* used in stomach content analysis (SCA), stable isotope analysis (SIA), and fatty acid analysis (FAA) in this study. F: female; M: male; I: immature; MA: maturing and matured. The same individuals were used for the 3 methods; size range: 195–380 mm

		SCA	SIA	FAA
Total		96	102	40
Sex	F	67	70	26
	M	29	32	14
Maturity	I	72	76	30
	MA	24	26	10

IV and V (mature). Beaks were dissected from the buccal masses and washed using deionized water for 5 min in an ultrasonic cleaner and stored in a glass bottle filled with 75% ethyl alcohol for measurement. The stomach of each specimen was removed and frozen (–80°C) after washing with 75% ethanol (empty stomachs were discarded). Approximately 2 × 2 cm bulk muscle tissue was taken from the area near the funnel-locking cartilage. Each piece of muscle tissue was washed using distilled water, freeze-dried at –55°C for at least 30 h (Martin Christ), and then ground to a fine powder and homogenized using a Retsch mixer mill MM 400 (Haan). Table 1 provides details of the number of samples analyzed for each method.

2.2. Morphometric analysis

Beaks were measured using a Vernier caliper with an accuracy of 0.01 mm following the procedure reported by Fang et al. (2015) (Fig. S1 in the Supplement at www.int-res.com/articles/suppl/m692p081_supp.pdf). In total, 12 morphometric variables were measured. The arms can be described and sequenced on one side due to the symmetrical body structure. Thus, the length of arms and tentacles to the nearest 1 mm was measured on only one side (Fig. S2) (Gong et al. 2018b). In this study, the preference was to measure the right-hand side of each specimen.

2.3. Stomach content analysis and DNA barcoding

Each stomach sample was defrosted and dissected, and the contents were visually sorted after being removed from the stomach and screened through a 150 µm mesh sieve. The prey categories, including fish sagittal otoliths, cephalopod beaks (sometimes sucker rings), and crustaceans, were identified to the lowest possible taxonomic level under a dissecting microscope (Olympus SZX7) consulting published references. The number of individuals consumed is reported based on the identifiable exoskeleton of crustaceans, the maximum number of upper or lower beaks for cephalopods, and the maximum number of left or right sagittal otoliths for fish. Frequency of occurrence (%FO) and numeric methods were used to quantify the diet. %FO was calculated as the percentage of squid that fed on certain prey. The number of individuals of a certain prey is reported relative to the total number of individual prey (%N). We did not include copepods within prey items in the analyses because they were too numerous and not directly consumed. However, we calculated the %FO of copepods since we wanted to get some useful information, such as the depth of feeding activities.

To complement visual SCA, we combined morphological identification with molecular methods to identify as many important prey species as possible that might have been missed by traditional methods. Prey pieces with less erosion that were excised from the muscle or mantle tissue of prey items were repeatedly rinsed with sterilized distilled water, 95% alcohol solution, and phosphate-buffered saline solution to avoid DNA cross-contamination. DNA was extracted via marine animal tissue columns (Guangzhou Dongsheng Biotech) following the manufacturer's protocol. The cytochrome *c* oxidase subunit I region of the mitochondrial genome was amplified using primers LCO1490 (forward) and HCO2198 (reverse) for DNA samples. For DNA samples that could not be amplified by these primers, mlCOIintF and mlCOIintR were used to increase the amplification rates of the prey sequences. The primers and PCR thermal cycle regime are shown in Table 2. Each 25 µl reaction included 5 µl of DNA, 0.5 µl of each primer, 12.5 µl of Ex Taq™ (2×; TaKaRa), and 6.5 µl of nanopure water.

The PCR products were run on 1% agarose gel, and amplification success was defined as a single intense band around 600 bp for the LCO1490 and HCO2198 primers or 300 bp for the mlCOIintF and mlCOIintR primers. The successful PCR products were sent to Sangon Biotech for purification and single-direction sequencing. Sequences were compared with public databases using the basic local alignment search tool on the National Center for Biotechnology Information server (http://www.ncbi.nlm.nih.gov/blast) and with reference to information about species composition in the sampling area.

Table 2. PCR primers and condition information

Name	Primer sequence (5′–3′)	PCR conditions	Reference
LCO1490 HCO2198	GG TCA ACA AAT CAT AAA GAT ATT GG TAA ACT TCA GGG TGA CCA AAA AAT CA	Initial denaturation for 6 min at 96°C, 33 cycles of 30 s at 94°C, 30 s at 55°C, and 40 s at 72°C, with a final cycle of 20 min at 72°C	Folmer et al. (1994)
mlCOIintF mlCOIintR	GGW ACW GGW TGA ACW GTW TAY CCY CC GGR GGR TAS ACS GTT CAS CCS GTS CC	Initial denaturation at 5 min at 95°C, 16 initial cycles of denaturation at 95°C for 10 s, annealing for 30 s at 56°C (–1°C per cycle), and extension at 72°C for 1 min followed by 25 cycles of denaturation at 95°C for 10 s, annealing at 46°C for 30 s, extension at 72°C for 1 min, and a final elongation for 10 min at 72°C	Leray et al. (2013)

2.4. Stable isotope determination

Powdered samples were weighed to approximately 1.00 mg with a precision balance (Excellence XPR microbalance, Mettler Toledo) and stored in a tin capsule for SIA. Bulk $\delta^{13}C$ and $\delta^{15}N$ were determined using an IsoPrime 100 isotope ratio mass spectrometer and a Vario Isotope Cube elemental analyzer (Elementar Analysensysteme) in the stable isotope laboratory of Shanghai Ocean University. Stable isotope ratios are reported in the delta (δ) notation and are expressed relative to the international standard, which is Vienna Pee Dee Belemnite for ^{13}C and atmospheric N_2 (air) for ^{15}N. Reference materials (protein [$\delta^{13}C$ = –26.98‰ and $\delta^{15}N$ = 5.94‰]) were used to calibrate the $\delta^{13}C$ and $\delta^{15}N$ results. Instrument SDs were 0.05 and 0.06‰ for the $\delta^{13}C$ and $\delta^{15}N$ measurements, respectively.

2.5. FA determination

Approximately 200 mg of powdered sample was weighed and placed in a 15 ml centrifuge tube with 12 ml 2:1 (v:v) chloroform:methanol and soaked for more than 20 h to extract the total lipids. The following steps were performed according to Gong et al. (2018a). The final upper organic layer (FA methyl esters [FAMEs] in *n*-heptane) was collected in a 1.5 ml sample bottle for FA composition analysis by a 7890B gas chromatograph interfaced with a 5977A single-quadrupole mass spectrometer (both from Agilent). FAMEs were identified according to FAME peaks determined by retention times as well as with comparison of the mass spectrum of unknown reference standards (GLC37, Nu-Chek Prep). Quantification was based on response factors determined by each FA in the standards relative to internal standards (C19:0, methyl nonadecanoate). FA results are reported as percentages of the total FAs and are grouped as saturated FAs (SFAs), monounsaturated FAs (MUFAs), and PUFAs.

2.6. Statistical analysis

2.6.1. Morphological ontogenetic breakpoints

To explore the breakpoints of morphological features during the ontogeny of *Dosidicus gigas*, pairwise linear regressions were performed according to the methods proposed by Kováč et al. (1999) and Vasconcellos et al. (2018). Twenty (except ML) mensural variables including FL and FW, 12 beak morphological data variables, and 6 data variables of arm and tentacle length were plotted against ML. The breakpoint is the abrupt transition of morphological features against the ML, which means a different growth pattern between the morphological attribute and the ML. Thus, we could use this method to separate squid size classes.

2.6.2. Effect factors

PERMANOVAs based on a Euclidean distance matrix were performed on the untransformed data of prey composition, stable isotope, and FA profiles of muscle separately to test the effects of size (ML), sex (female or male), and maturity (immature or mature),

because PERMANOVA could provide robust testing of unbalanced and dispersed datasets. It does not require normal distribution of data. Moreover, untransformed data were used to avoid lending artificial weight to the small quantities of data (Kelly & Scheibling 2012, Anderson & Walsh 2013, Young et al. 2018).

2.6.3. SCA

A randomized cumulative prey curve was generated to evaluate sample size using the lowest taxonomic level of each prey. The last 4 points were taken and fitted to a straight line. A chi-square statistic (χ^2 test) was applied to compare the slope of this line to a line of slope zero (α = 0.05). The sample size was considered adequate when there was no significant difference in the slopes of the 2 lines.

Squid heavily masticate their food and have rapid digestion rates. Thus, prey rapidly becomes a complex slurry that cannot be uniquely assigned to any given prey species, especially when multiple species are present in a single stomach. This prevents the accurate assignment of a percentage of weight or mass to a given species using traditional methods (weight or volume estimation of mass). Consequently, the index of relative importance, which is the most common index, does not apply to this study. Instead, the geometric index of importance (GII) was used:

$$GII_j = \frac{(\%N_j + \%FO_j)_j}{\sqrt{2}}$$

where j represents the j^{th} prey category.

The diet diversity of each squid species was examined using the Shannon-Wiener index ($H = -(\sum P_i \times \ln P_i)$, where P_i represents the abundance proportion of prey i in each sample). Samples were grouped in 20 mm ML intervals. The %FO of the copepod, zooplankton (except copepod), fish, cephalopod, and the top 4 or 5 prey items of each category was calculated in each size group.

2.6.4. SIA

Stable isotope values were integrated by size groups based on 10 mm ML intervals to investigate the variations in $\delta^{13}C$ and $\delta^{15}N$ with increasing ML. Variations in $\delta^{13}C$ and $\delta^{15}N$ between size classes were investigated using ANOVA.

2.6.5. FAA

FA profiles were integrated by size groups in 25 mm ML intervals, which were divided into 7 size groups. The 7 sizes were grouped using cluster analysis based on Ward's minimum variance method. ANOVA was performed on each FA between size classes.

2.6.6. Trophic niche

Non-metric multidimensional scaling (NMDS), based on the Euclidean distance matrix, was used to compare the prey composition and FAs of the size groups in 2 dimensions. ANOSIM was performed to determine similarity in the FAs of different size groups, and the FAs that contributed most to the observed differences in the percentage composition of *D. gigas* between size groups were evaluated using SIMPER.

Trophic niche, expressed as a convex hull integration of organisms positioned at the edge of SCA, SIA, or FAA datasets, allowed the area to be compared and the species-specific indices of nestedness, defined as the ratio between the overlap area and the smallest volume of the convex hull (Cucherousset & Villéger 2015), to be measured. The index of nestedness ranges from 0 to 1, indicating no overlap to complete overlap of the minimum volume in a larger hull. Each stable isotope and x and y coordinate of the NMDS analysis of stomach contents and FAs were scaled to have the same range (isotopic nestedness; Cucherousset & Villéger 2015), allowing us to quantify the feeding niche occupied by each size group as well as to compare information derived from SCA, SIA, and FAA. In addition, the Bayesian method SIBER (stable isotope Bayesian ellipse in R) was complementary to calculate the corrected standard ellipse area (SEAc) and overlap of trophic niche between different size groups (Jackson et al. 2011). The SEAc was set to contain 40% of observation data, focusing on characterizing the center of the trophic niche, and is not influenced by sample size or outliers, while the traditional convex hull area (total area) involves all individual values, integrating the importance of the organism located at the edge of the trophic niche. The combination of the convex hull and Bayesian ellipse could provide a multiperspective characterization of the trophic niche (Jackson et al. 2011, Cucherousset & Villéger 2015).

All statistical analyses were conducted using R v. 3.5.3 (R Core Team 2019). For ANOVA and SIM, all

Table 3. Breakpoints from piecewise regression models adjusted to the growth of the morphological characteristics of beaks, tentacles, and fin length (FL) versus mantle length (ML) (n = 379). FW: fin width; UHL: upper hood length; UCL: upper crest length; URL: upper rostrum length; URW: upper rostrum width; ULWL: upper lateral wall length; UWL: upper wing length; LHL: lower hood length; LCL: lower crest length; LRL: lower rostrum length; LRW: lower rostrum width; LLWL: lower lateral wall length; LWL: lower wing length; TL: tentacle length; CL: tentacular club length; A1–A4: 4 arms for 1 side. Schematics are shown in Figs. S1 & S2

Type	Variable	Regression 1		Break-point	Regression 2	
		Slope 1	Intercept 1		Slope 2	Intercept 2
Fin	FL	0.373	7.314	261.99	0.616	−69.144
	FW	0.661	4.530	251.00	0.782	−25.749
Beak	UHL	0.071	−1.668	257.05	0.091	−6.859
	UCL	0.088	−1.543	259.00	0.101	−4.943
	URL	0.016	1.674	255.99	0.028	−1.507
	URW	0.015	1.650	251.00	0.022	−0.118
	ULWL	0.046	3.051	246.98	0.077	−4.693
	UWL	0.014	1.323	252.30	0.022	−0.767
	LHL	0.008	2.679	250.42	0.022	−0.769
	LCL	0.036	0.682	255.01	0.044	−1.362
	LRL	0.015	1.514	254.99	0.025	−1.020
	LRW	0.016	1.428	255.62	0.024	−0.744
	LLWL	0.050	2.148	249.00	0.072	−3.243
	LWL	0.010	4.898	247.00	0.045	−3.651
Tentacles and arms	TL	0.812	84.518	250.03	0.782	−25.749
	CL	0.417	5.968	249.99	1.272	−30.546
	A1	0.516	−2.076	246.14	0.701	−65.152
	A2	0.490	18.981	246.36	0.691	−44.985
	A3	0.402	42.991	244.00	0.723	−38.487
	A4	0.395	23.353	239.00	0.692	−27.655

variables were checked for normality and homogeneity of variance, using Shapiro-Wilk and Levene tests, respectively, where necessary, arcsine square-root transformed before further statistical analysis.

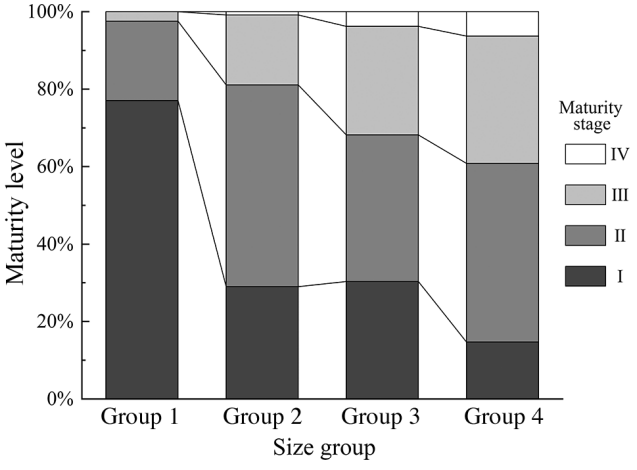

Fig. 2. Proportion (as %) of maturity levels of the 4 size groups. Gonad maturity stages are defined by Arkhipkin & Laptikhovsky (1994). I: immature; II: immature; III: maturing; IV: mature

3. RESULTS

3.1. Size groups based on breakpoints

A total of 379 squid specimens were sampled for morphometric analysis. MLs ranged from 195 to 380 mm. According to the results of piecewise regression models, all breakpoints were detected within 239 to 262 mm (Table 3, Fig. S3). According to the range of detected breakpoints (or we could also call them 'growth inflections') in each type of morphological characteristic, we identified 3 important turning points, which were 239, 250, and 262 mm. Hence, *Dosidicus gigas* specimens were divided into 4 size groups: Group 1 with ML < 239 mm, Group 2 with ML ranging from 239 to 250 mm, Group 3 with ML ranging from 251 to 262 mm, and Group 4 with ML > 262 mm.

3.2. Gonad development

The maturity level proportions of the 4 size groups, expressed as percentages, are shown in Fig. 2. In Group 1, *D. gigas* was almost at maturity stage I, and the percentage of immature squid specimens was 97%. Groups 2 to 4 showed a period of gonad development (maturity ratios ranged from 19 to 37%), indicating an increase in maturity trends across the 4 size groups. A clear relationship was found between squid size and maturity stage, indicating that size is, to some extent, a proxy for ontogenetic processes.

3.3. Diet

In total, 96 stomachs of *D. gigas* were dissected and their contents statistically analyzed. The cumulative prey curve suggested the sample size is sufficient to describe the diet (p = 0.651) (Fig. S4). The diet comprised 73 prey categories, including 6 gastropods, 16 crustaceans, 1 bivalve, 36 fishes, and 14 cephalopods. Taxonomic assignments, %FO, %N, GII, and rank of GII are reported in Table S1. Only the %FO of copepods was calculated due to their large numbers and because they are usually the prey of small pelagic fishes. According to the GII, the top 6 included (in descending order) *Vinciguerria lucetia*

Table 4. Prey items represented by L1 to L6. L1 indicates the 4 categories (copepod, zooplankton except copepod, fish, and cephalopod); L2 to L6 represent the top 5 most frequently occurring prey items

	Copepod	Zooplankton	Fish	Cephalopod
L1	Total	Total (except copepod)	Total	Total
L2		*Heliconoides* sp. 1	*Vinciguerria lucetia*	*Dosidicus gigas*
L3		Nuculidae	*Vinciguerria lucetia* larvae	*Abraliopsis tui*
L4		*Hyperioides longipes*	*Sternoptyx diaphana*	*Gonatus madokai*
L5		*Phronima sedentaria*	*Diogenichthys laternatus*	*Symlectoteuthis oualaniensis*
L6			Fish larvae	

(GII = 95.93), *Heliconoides* sp. (GII = 59.88), *Sternoptyx diaphana* (GII = 58.12), *Diogenichthys ernatus* (GII = 54.72), *V. lucetia* larvae (GII = 43.64), and *D. gigas* (GII = 33.71). We found a significant relationship in the dietary composition with size according to variance contribution but not between sexes and maturity (Table S2).

Prey items were classified into 4 main categories (copepod, zooplankton except copepod, fish, and cephalopod) as shown in Table 4. In terms of the latter 3 categories, the 5 most frequently occurring prey items were used in further analysis. In general (line L1), we observed that the %FO of copepods and other zooplankton (gastropods, bivalves, and crustaceans) showed a trend of decreasing and then increasing with increasing ML in the sample size range in this study. In contrast, the frequency of fish showed less fluctuation, and cephalopods showed a slightly increasing trend (Fig. 3, Table 4). %FO of *D. gigas* cannibalism (cephalopod line L2) increased

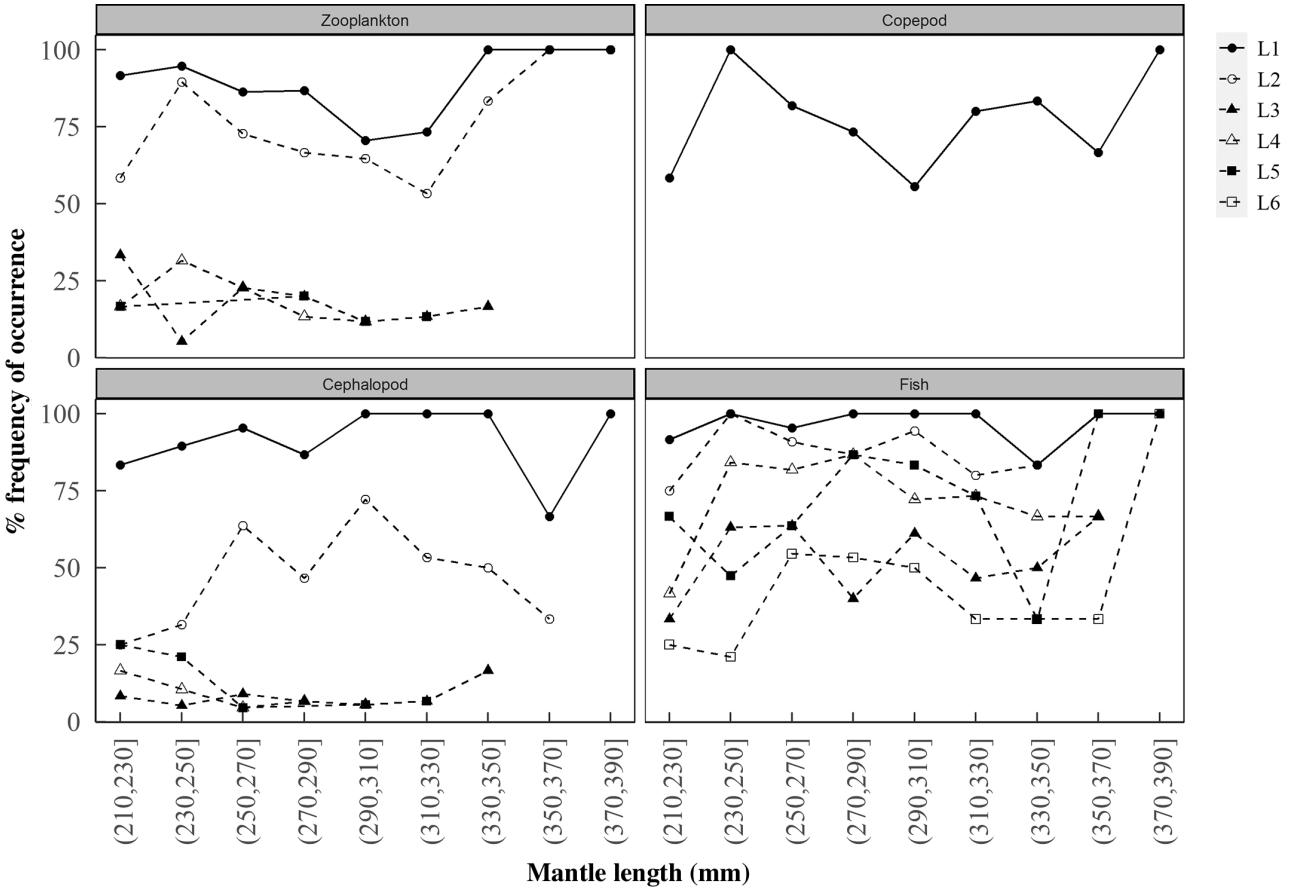

Fig. 3. Variability in the feeding of *Dosidicus gigas* of different sizes from the eastern Pacific (frequency of occurrence). L1 to L6 are defined in Table 4. Numbers in brackets indicate the mantle length range in each size group, e.g. (210, 230] = >210 to 230. Similar for all size ranges here and in the following diagrams

with increasing ML, with a sharp increase after 250 mm. However, the frequency curve started to decrease at ML > 310 mm, accompanied by an increase in the %FO of copepods and *Heliconoides* sp. 1 (zooplankton line L2). Although *D. gigas* changes from a predator of planktonic larvae to a predator of nekton during its ontogenesis, a large amount of plankton (copepod, gastropod) was still found in large individuals.

The Shannon diversity index increased and then decreased with ML, showing a trend similar to a normal distribution. The Shannon diversity index increased apparently when ML was >250 mm but decreased significantly at ML >310 mm (Fig. 4).

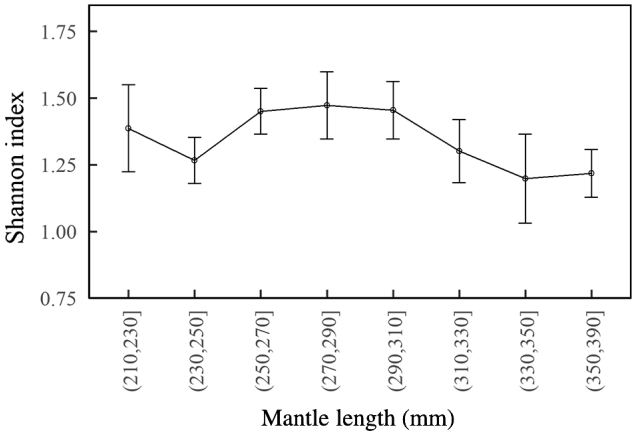

Fig. 4. Variability in the Shannon index (mean ± SD) of different size groups. Numbers in brackets indicate the mantle length range in each size group

3.4. Stable isotope values and FA profiles

According to the PERMANOVA results, $\delta^{13}C$ differed significantly with size, and $\delta^{15}N$ differed significantly with both size and sexual maturity stage (Table S3). $\delta^{13}C$ decreased significantly after ML reached 251–260 mm. $\delta^{15}N$, although fluctuating, also showed a significant decrease in ML between 251–260 and 310–320 mm (Fig. 5).

PERMANOVA results showed significant size-related (ML) differences in the FA profiles ($p < 0.01$) (Table S4). Based on the clustering results of FA composition, size groups were divided into 2 groups: the first group included 3 sizes (201–225, 226–250, and 301–325 mm), and the second group included 4 sizes (251–275, 276–300, 326–350, and 351–375 mm) (Fig. 6).

The results of the above analysis showed that *D. gigas* undergoes at least 1 dietary shift during its growth, and the period of dietary shift is at ~250 mm ML. Therefore, to more intuitively evaluate the trophic niche transformation with *D. gigas* growth, the organisms were merged into 2 main groups: Group I for ML ≤ 250 mm and Group II for ML > 250 mm.

Twenty-eight FAs were detected in *D. gigas* muscle, consisting of 10 types of SFAs, 8 MUFAs, and 10 PUFAs (Table S5). The most abundant FAs in *D. gigas* were PUFAs followed by SFAs and MUFAs. Significant differences were detected in the comparative content for most FAs between the 2 groups. The total amount of SFAs in Group I (32.08 ± 0.6%) was significantly higher than that in Group II (31.16 ± 1.18%, ANOVA, $F(1,38) = 8.64$, $p < 0.01$), whereas ΣMUFAs had the opposite result in Group I (8.41 ± 0.78%) and were significantly lower than those in Group II (9.86 ± 1.12%, ANOVA, $F(1,38) = 20.761$, $p < 0.01$). No significant difference was observed in ΣPUFAs (ANOVA, $F(1,38) = 2.61$, $p = 0.115$). Both $\delta^{13}C$ and $\delta^{15}N$ showed significant differences between the 2 groups (ANOVA, $\delta^{13}C$: $F(1,100) = 11.80$, $p < 0.001$; $\delta^{15}N$: $F(1,100) = 7.47$, $p < 0.01$), and the range of Group II ($\delta^{13}C$: –19.27 to

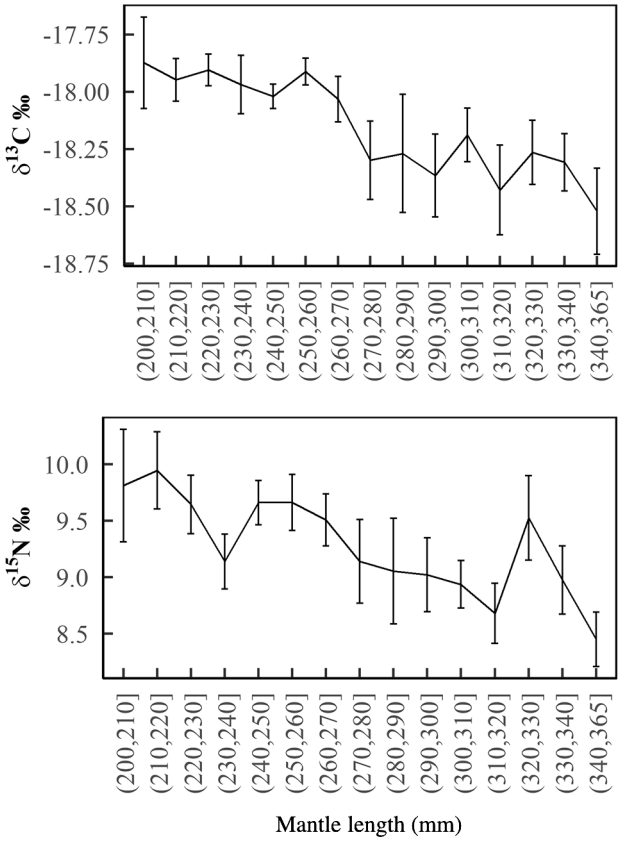

Fig. 5. Variability in the stable isotope ($\delta^{13}C$ and $\delta^{15}N$) values (mean ± SD) of each size group. Numbers in brackets indicate the mantle length range in each size group

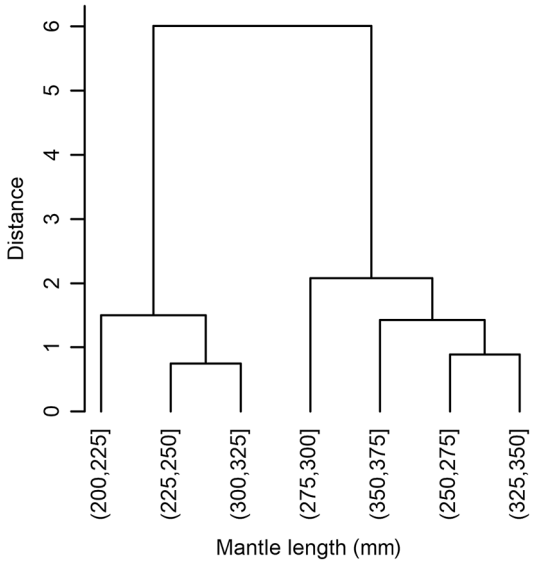

Fig. 6. Cluster analysis of fatty acid profiles in different size groups. Numbers in brackets indicate the mantle length range in each size group

Table 5. Convex hull area (total area [TA]) and corrected standard ellipse area (SEAc) values (‰^{2}) for Groups I and II based on stomach content analysis (SCA), stable isotope analysis (SIA), and fatty acid analysis (FAA)

	TA		SEAc	
	Group I	Group II	Group I	Group II
SCA	0.243	0.734	0.071	0.168
SIA	0.183	0.384	0.061	0.118
FAA	0.151	0.397	0.060	0.158

Table 6. Indices of similarity and nestedness between Groups I and II calculated using the method of Cucherousset & Villéger (2015) based on stomach content analysis (SCA), stable isotope analysis (SIA), and fatty acid analysis (FAA)

	Similarity	Nestedness
SCA	0.309	0.951
SIA	0.378	0.852
FAA	0.174	0.537

–17.65‰; δ^{15}N: 1~10.83‰) was broader than that of Group I (δ^{13}C: –18.45 to –17.59‰; δ^{15}N: 8.32~10.94‰). The δ^{15}N values were more variable than the δ^{13}C values (Table S5).

3.5. Trophic niche partitioning

To reduce bias from testing error and unidentified FAs, only FAs with a comparative content greater than 1% were selected for comparisons between the 2 groups, which comprised C16:0, C17:0, C18:0, C18:1n9, C20:1n9, C20:3n3, C20:4n6, C20:5n3, C22:2n6, and C22:6n3. Both the convex hull and Bayesian standard ellipse trophic niche metrics of size groups overlapped according to prey composition, isotopic, and FA data. According to the results, niche areas based on the prey composition (in number) of Groups I and II were 0.243 and 0.734 for the convex hulls and 0.071 and 0.168 for the Bayesian standard ellipses, respectively (Table 5, Fig. 7). The overlap index was 0.951(nestedness) for the convex hull, and the mean overlap value was 0.315 for the standard ellipse (Table 6, Fig. 8). In the isotopic niche metric, the convex hull area was 0.183 and 0.384 for Groups I and II, respectively, and the calculated SEAc was 0.061 and 0.118 for Groups I and II, respectively (Table 5, Fig. 7). The isotopic feeding niches of the 2 size groups overlapped with an isotopic nestedness of 0.852, while the estimated rate of ellipse overlap was 0.359 (Table 6, Fig. 8). The FA trophic niche had the smallest overlap of the above 2 methods, which had a nestedness value of 0.537 based on the convex hull and 0.175 for the Bayesian standard ellipse (Table 6, Fig. 8). Simi-

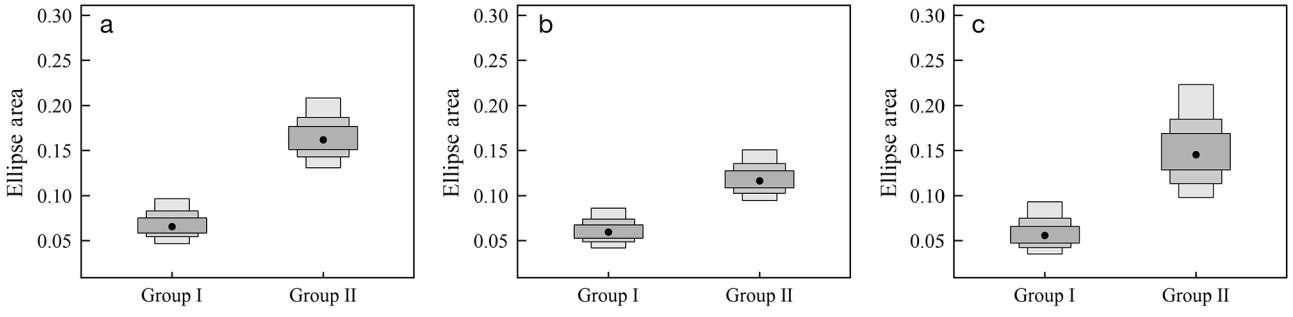

Fig. 7. Corrected standard ellipse area (SEAc) of Group I (mantle length ≤250 mm) and Group II (mantle length >250 mm) based on (a) non-metric multidimensional scaling (NMDS) dimensions of the prey composition (in number), (b) stable isotope (δ^{13}C and δ^{15}N) values of muscle, and (c) NMDS dimensions of the fatty acid profiles of muscle

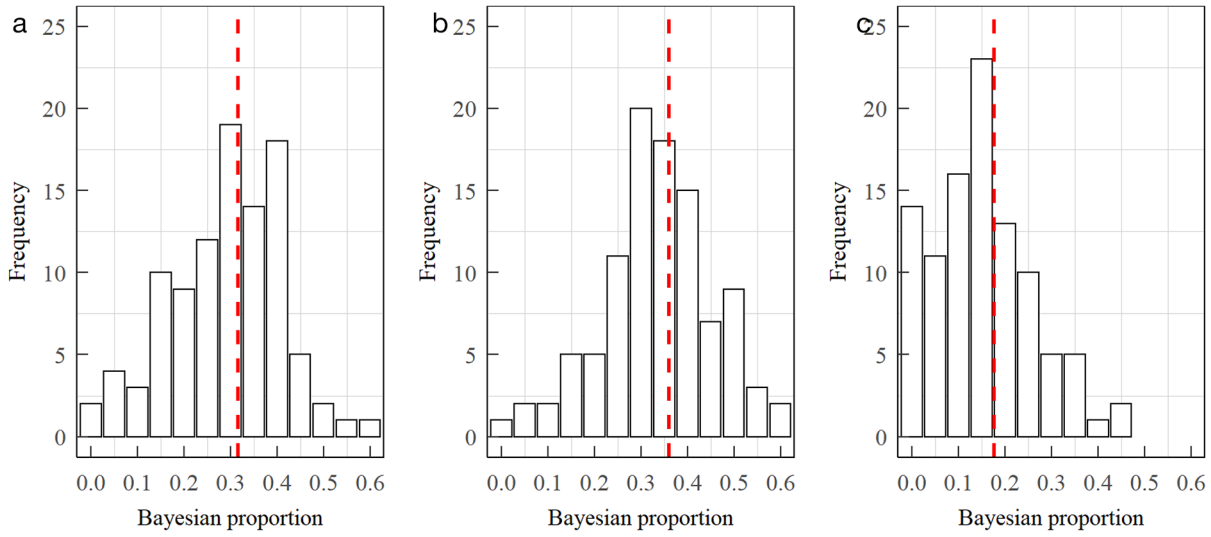

Fig. 8. Pairwise comparison of Bayesian ellipse overlaps between Groups I and II based on Bayesian model. (a) Dietary niche; (b) isotopic niche; (c) fatty acid niche. Red dashed lines indicate mean values

larly, the FA niche area of Group I was 0.151 and 0.060 for the convex hull and standard ellipse, respectively; for Group II, the area of the FA trophic niche was 0.397 0.158 for the convex hull and standard ellipse, respectively. In general, the prey composition, stable isotope, and FA tracers showed the same trend that the extent of the trophic niches was larger for Group II than for Group I.

3.6. Intraspecific differences in FA profiles

ANOSIM showed significant differences in the FA composition of the 2 size groups (p = 0.011, R = 0.131), which revealed shifts in the diets with growth.

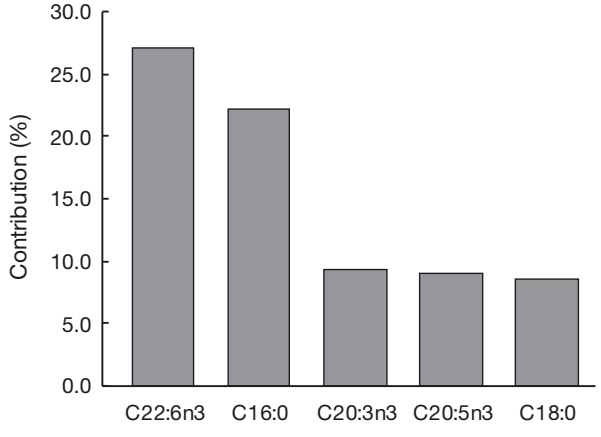

Fig. 9. Contribution of primary fatty acids in *Dosidicus gigas* muscle tissue causing the differences between size groups in SIMPER analysis

According to SIMPER (Fig. 9), C22:6n3 and C16:0 were most influential as distinguishers for the 2 size groups (the cumulative percentage contribution of C22:6n3 and C16:0 was 49.3%: 27.1% for C22:6n3 and 22.2% for C16:0). C20:3n3, C20:5n3, and C18:0 were the next main FAs that influenced the differences, with percentage contributions of 9.3, 9.0, and 8.5%, respectively.

4. DISCUSSION

Based on the morphometric analysis, SCA, SIA, and FAA of *Dosidicus gigas* in the eastern equatorial Pacific, differences in trophic ecology and feeding strategies along growth were examined, reflecting that equatorial *D. gigas* undergo an ontogenetic diet shift at ~250 mm ML. Information on the trophic ecology of *D. gigas* provided in our study can not only give insight into the pattern of resource use affected by individual ontogeny, but also allow for a deeper understanding of the mechanisms underlying the high productivity of the *D. gigas* population. In addition, further research on the dynamics of their resource utilization in response to environmental variability will aid in the sustained use of this fishery resource.

4.1. Breakpoints of feeding organs

How marine animals use food resources can be influenced by the size, morphology of their feeding

apparatus, swimming ability, habitat environment, and food type (Vasconcellos et al. 2018). Early ommastrephid squids have a detritus-based diet, which allows them to take advantage of almost ubiquitous and accessible food resources and thus minimize the degree of competition within a species (Fernández-Álvarez et al. 2018). Coupled with continuous growth, ommastrephids have been found to shift their diet from small epipelagic plankton to crustaceans, mollusks, and fishes, which are larger and which provide more energy (Markaida & Sosa-Nishizaki 2003, Fernández-Álvarez et al. 2018). This shift is always accompanied by changes in morphology, such as the formation of 2 independent raptorial tentacles and the emergence of the hard and sharp beak. Variations in morphology are usually linked to feeding structure, feeding behavior, swimming ability, and habitat environment, leading to feeding on different food types (Hourston et al. 2004). Hence, the morphological features of cephalopods can indicate feeding strategies and therefore different niches (Ventura et al. 2017).

In this study, we used linear piecewise (split) regression models to explore the breakpoints of the important feeding morphological features along growth. The results showed that morphological variables were positively correlated with ML. Twenty morphological features showed a turning point against the ML. Not all the breakpoints were detected at the same ML, but were detected in a relatively narrow range from 239 to 262 mm ML. Therefore, there may be a turning point in feeding habits for *D. gigas* related to the development of the feeding apparatus.

4.2. Ontogenetic dietary shift

PERMANOVA results showed that the size of *D. gigas* had a significant effect on its prey composition, stable isotope values, and FA profiles. Sexual maturity only had a significant effect on $\delta^{15}N$, whereas sex had no significant effect on any of these 3 variables. Therefore, the body size of *D. gigas* was considered a key factor affecting its feeding habits, in agreement with the results of Portner et al. (2020). The %FO of zooplankton and cephalopods in the prey items changed with the increase in the size of *D. gigas* individuals. The %FO of cephalopods increased gradually with ML when ML > 250 mm, but after ML > 310 mm, these larger individuals seemed to prefer feeding on zooplankton at lower trophic levels. Similar contrasting results related to the SIAR outputs were described for *D. gigas* in the North Pacific, showing macrozooplankton as one of the most important prey of *D. gigas* (Miller et al. 2013). This feature was also reflected in the FA profiles; that is, individuals with an ML of 301–325 mm had a more similar FA profile to 225–250 mm individuals. This may be related to the optimal foraging theory proposed by MacArthur & Pianka (1966), which states that predators maximize the difference between their energy gain from food and the cost of consumption required to forage, maximizing their net energy gain. Although smaller prey have a relatively low energetic value, predators consume less energy to feed on and process them, whereas larger prey are harder to capture and their processing time is longer; therefore, predators may need to consume more energy in their predation. Scharf et al. (2000) also suggested that the selection of smaller prey items can increase predation efficiency. In addition, predation on small food can effectively reduce competition for resources with similarly sized fish species (Field et al. 2013). Cannibalism was also found in *D. gigas* in equatorial waters and showed an increasing and then decreasing trend with increasing ML. This behavior may be an important method for cephalopods to obtain energy, which can provide advantages in terms of food competition for large individual predators (which usually feed on smaller conspecifics). Cannibalism can also improve survival in times of food shortage (Caddy 1983) and is associated with an increased ability to capture and process prey, allowing larger individuals to obtain more energy (Christensen 1996, Lundvall et al. 1999). However, the frequency of cannibalism in *D. gigas* decreased after ML > 310 mm, which may be related to their relative spatial separation from smaller indiuals (discussed below) (Trasviña-Carrillo et al. 2018). Because *D. gigas* is an opportunistic predator, it is difficult to observe the key points of feeding transitions during their growth, which need to be determined in conjunction with stable isotope values and FA profiles of muscle.

Stable isotope values can be used to infer the food source and trophic level of consumers, reflecting information about consumers' dietary intake during a certain period (Post 2002). The fluctuations in $\delta^{13}C$ and $\delta^{15}N$ with the ML of *D. gigas* can reflect the changes in diets and migration patterns during their growth. When ML ≤ 260 mm, the variation in $\delta^{13}C$ values was relatively smooth, suggesting specific habitats and food sources (Trasviña-Carrillo et al. 2018); when ML > 260 mm, $\delta^{13}C$ showed large fluctuations and decreased significantly with increasing ML, indicating a large change in their food sources and migration. Compared to $\delta^{13}C$, $\delta^{15}N$ has a greater

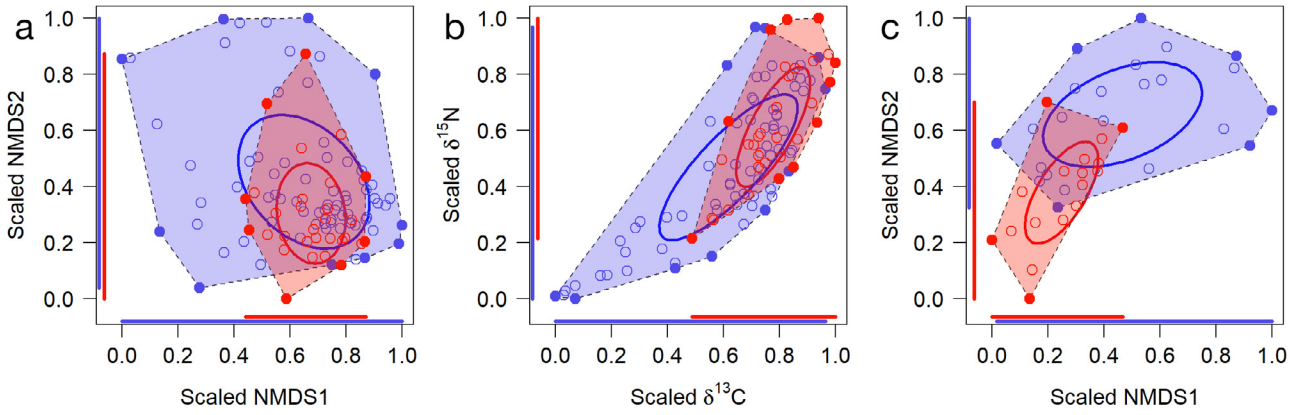

Fig. 10. Trophic niches of Group I (mantle length ≤250 mm; red) and Group II (mantle length >250 mm; blue) from the central equatorial Pacific Ocean based on (a) non-metric multidimensional scaling (NMDS) dimensions of prey composition (in number), (b) stable isotope ($\delta^{13}C$ and $\delta^{15}N$) values of muscle, and (c) NMDS dimensions of the fatty acid profiles of muscle. Trophic niche widths are represented by polygons and Bayesian standard ellipses

tendency to fluctuate, which may be related to $\delta^{15}N$ having a wider variability across latitudes and trophic levels. It was reported that the variation in the $\delta^{13}C$ increase is 0 to 1‰, whereas the variation in $\delta^{15}N$ is 2.5 to 3.4‰ per trophic level (Post 2002). The variation in $\delta^{13}C$ values in the muscle of *D. gigas* at different latitudes is approximately 4.0‰, whereas the variation in $\delta^{15}N$ values is approximately 9.0‰ (Argüelles et al. 2012). Both $\delta^{13}C$ and $\delta^{15}N$ showed a decreasing trend with the growth of *D. gigas*, which may be related to its higher intake of lower trophic level organisms but may also indicate its possible migration from nearshore areas to the ocean (Alegre et al. 2014, Li et al. 2017). Evidence demonstrated that *D. gigas* grows and feeds nearshore and migrates to pelagic spawning areas with lower levels of primary productivity in summer and winter. This behavior may reduce the risk of predation. The proportion of mature individuals and prey items at low trophic levels (e.g. crustaceans) increases as individuals grow during the migration from inshore to pelagic areas in *D. gigas*, consistent with our results (Argüelles et al. 2012). Thus, the segregation in the spatial and feeding habits of different sizes of *D. gigas* may be a mechanism for their avoidance of predation and cannibalism.

Although all these techniques can describe the feeding ecology of a given species, each one provides its own insights. Stomach contents indicate detailed prey composition, and isotopic values help to define productivity sources and migrations, whereas FAs indicate finer-scale spatial heterogeneity in diets and provide insight into energy metabolism. Our experimental results showed that PUFAs constituted the majority of the FAs of *D. gigas*, followed by SFAs and MUFAs (Table S5). These findings agree with a previous observation: C22:6n3 (docosahexaenoic acid [DHA]) and C16:0 were identified as major concentrated components in *D. gigas*, which indicated that PUFAs and SFAs are storage lipids that can potentially supply energy for activity (Henderson et al. 1984, Saito et al. 2014, Gong et al. 2018a). A significant shift was observed in the FA trophic niches with size groups (Fig. 10c), and DHA and C16:0 were identified as the primary drivers of the variation in the FA profiles (Fig. 9). The higher FA percentage of Group I may reflect growth shifts in response to changes in food resource availability and energy allocation. This is because DHA cannot be synthesized by high trophic level predators; therefore, these predators must rely on dietary sources (Iverson et al. 2004). In larger and deep-diver species, proportions of DHA were lower, corresponding to feeding on fewer pelagic organisms, as DHA is usually used as an FA marker for zooplankton as well as for dinoflagellates and cryptomonads (Kharlamenko et al. 2001). DHA is positively correlated with the reproductive state. Palmitic acid (C16:0) is the basic SFA and is certified as an essential FA for rapid growth and survival (Henderson et al. 1984, Nogueira et al. 2017). Larger individuals tend to have higher metabolic requirements and increased physical activity compared to smaller ones and consequently catabolize more of their muscle lipids (Henderson et al. 1984). Chen et al. (2020) suggested that *gigas* continuously feed during their growth and maturation; their reproduction investment tends to mostly rely on continual food intake. Furthermore, the energy stored in muscle tissues is partially converted to use for reproductive development and

metabolism (Chen et al. 2020). It would be reasonable to assume that larger individuals with a wider niche breadth probably have more active and voracious feeding activity than smaller ones. Larger squids need to consume more energy to forage and for gonadal development (reproduction), consistent with the maturity of the gonad with growth (Fig. 2). Moreover, the proportion of MUFAs for Group II was significantly higher than that for Group I, supporting the idea that larger individuals feed on deeper prey, as MUFAs are rich in mesopelagic prey or in fish such as myctophids that feed on mesopelagic copepods (Nesis 1970, Shetinnikov 1989, Saito & Murata 1998, Teuber et al. 2014).

According to the ML growth curves with age for *D. gigas* in the eastern equatorial Pacific Ocean calculated by Liu et al. (2017), when ML is 250 mm, the corresponding age of *D. gigas* is 156 to 157 d, which is at the end of the juvenile stage or the beginning of the adult stage (Xu et al. 2019). Therefore, the shift in the diet of *D. gigas* may occur with the development of the feeding apparatus, increased swimming ability, and accelerated metabolism during the transition from the juvenile to the adult stage.

4.3. Trophic niche partitioning

We used a multiple-indicator dietary assessment to describe intraspecific interactions through direct and assimilated diet information. SCA reflects a snapshot of the food predated for a short time (usually <24 h), while biochemical tracers reflect the diet assimilation for several weeks to a month. Compared to FA, stable isotopes have a relatively longer turnover rate (Pethybridge et al. 2018).

The overlap analyses of FA niche appear to indicate that Group II individuals exploit different prey resources than Group I. However, SIA and SCA niches showed a large overlap (Fig. 10a,b), mainly due to similar isotopic baselines and prey composition in the study area. Besides, it seems the incidental prey identification for SCA and longer turnover rates weakened the ability of stable isotopes to depict diet differentiation.

The niche area of species in Group II was approximately 2 times larger than that of Group I (Fig. 10), which had wider ranges in both $\delta^{13}C$ and $\delta^{15}N$, indicating that *D. gigas* may use a wider range of resources. However, the trend in the Shannon diversity index did not seem to support this result, which showed a significant decrease with increasing ML. Similar results were reported by Liu et al. (2020), who found that the area of the trophic niche of *D. gigas* is relatively narrow during the adult and mortality stages and suggested that this may be related to its reduced migratory range and food specialization. However, consumers' FA patterns could be also influenced by the changes in internal regulation during ontogeny and to some extent may act as a buffer for the differences between energy availability and physiological demands, which need to be further studied (Chaguaceda et al. 2020).

In this study, the decrease in the Shannon diversity index may be related to the diet specialization of larger individuals, which may reduce intraspecific competition between individuals. For example, some large individuals can ingest larger and isotopically enriched prey; as a result, they have a higher $\delta^{15}N$ (Nigmatullin et al. 2001, Ruiz-Cooley et al. 2006, Galván et al. 2010, Franco-Santos & Vidal 2014). However, other large individuals can also ingest small prey such as euphausiids and juvenile *Vinciguerria lucetia* at low trophic levels, but they are horizontally (spatially) isolated from smaller individuals (Ibáñez et al. 2008, this study). Expansion of the food range leads to expansion of the trophic niche of *D. gigas* (Franco-Santos & Vidal 2014, Trasviña-Carrillo et al. 2018, Jones et al. 2019). Another reason for the expansion of the niche width is that *D. gigas* presents vertical segregation by size (Trasviña-Carrillo et al. 2018). Larger individuals face larger temperature and habitat changes due to their vertical behavior, implying that such deep divers might change their dietary and habitat preferences since diving capacity increases with size due to fin development, which may allow the capture of a wide range of prey (Franco-Santos & Vidal 2014, Trasviña-Carrillo et al. 2018, Jones et al. 2019). The segregation of the vertical distribution of *D. gigas* forces them to reduce their metabolic rate and energy consumption and lower the risk of predation by top predators (Gilly et al. 2006, Rosa & Seibel 2010, Stewart et al. 2013, Trasviña-Carrillo et al. 2018). Therefore, *D. gigas* may apply different feeding and survival strategies during their growth, aiming to reduce the risk of predation and to optimize foraging energy costs to improve survival ability.

5. CONCLUSIONS

The combination of stomach contents, stable isotopes with FA biomarkers, and morphometric analyses is a powerful integrated approach that provides a comprehensive description of trophic structure and

dynamics. Our analyses showed that *Dosidicus gigas* exhibits ontogenetic variation in morphological characteristics and niche partitioning. Ontogenetic shifts in the diet may occur at ~250 mm ML, which probably reflects the combination of metabolic demand, swimming ability, and size or morphology of the feeding apparatus (arms, tentacles, and beak) with increasing body size. The choice of food and spatial segregation of different sizes of individuals can help reduce intraspecific competition. Therefore, morphology and energy metabolism must be considered when studying ontogenetic feeding ecology. Our study also indicates that multiple indicators in the dietary assessment are essential. However, our sampling lacked a robust representation across length classes to detect such early changes in *D. gigas*. Due to its extensive migration and flexible feeding strategy, it is hypothesized that it may undergo multiple dietary shifts during its lifetime. Thus, future work should focus on smaller and larger squid (<200 mm and >400 cm) to investigate ontogenetic changes in foraging strategies.

Acknowledgements. This work was funded in part by the National Natural Science Foundation of China (31872573, 31900333, and 41541042). We thank the volunteers of the College of Marine Sciences, Shanghai Ocean University, for their assistance with biological parameter measurements and sample collections in the lab. We thank Huiqiong Wang and Chunxia Gao for FA preparation and stable isotope measurement.

LITERATURE CITED

Alegre A, Ménard F, Tafur R, Espinoza P and others (2014) Comprehensive model of jumbo squid *Dosidicus gigas* trophic ecology in the northern Humboldt Current System. PLOS ONE 9:e85919

Anderson MJ, Walsh DCI (2013) PERMANOVA, ANOSIM, and the Mantel test in the face of heterogeneous dispersions: What null hypothesis are you testing? Ecol Monogr 83:557–574

Argüelles J, Lorrain A, Cherel Y, Graco M and others (2012) Tracking habitat and resource use for the jumbo squid *Dosidicus gigas*: a stable isotope analysis in the northern Humboldt Current System. Mar Biol 159:2105–2116

Arkhipkin AI, Laptikhovsky V (1994) Seasonal and interannual variability in growth and maturation of winter-spawning *Illex argentinus* (Cephalopoda, Ommastrephidae) in the southwest Atlantic. Aquat Living Resour 7: 221–232

Baeta A (2019) Stable isotope ecology. In: Faith B (ed) Encyclopedia of ecology, 2nd edn, Vol 3. Springer, Amsterdam, p 606–615

Bell JG, Ghioni C, Sargent JR (1994) Fatty acid compositions of 10 freshwater invertebrates which are natural food organisms of Atlantic salmon parr (*Salmo salar*): a comparison with commercial diets. Aquaculture 128:301–313

Caddy JF (1983) The cephalopods: factors relevant to their population dynamics and to the assessment and management of stocks. FAO Fish Tech Pap 231:416–449

Chaguaceda F, Eklöv P, Scharnweber K (2020) Regulation of fatty acid composition related to ontogenetic changes and niche differentiation of a common aquatic consumer. Oecologia 193:325–336

Chen X, Han F, Zhu K, Punt AE, Lin D (2020) The breeding strategy of female jumbo squid *Dosidicus gigas*: energy acquisition and allocation. Sci Rep 10:9639

Christensen B (1996) Predator foraging capabilities and prey antipredator behaviours: pre- versus postcapture constraints on size-dependent predator–prey interactions. Oikos 76:368

Cucherousset J, Villéger S (2015) Quantifying the multiple facets of isotopic diversity: new metrics for stable isotope ecology. Ecol Indic 56:152–160

Drazen JC, Phleger CF, Guest MA, Nichols PD (2009) Lipid composition and diet inferences of abyssal macrourids of the eastern North Pacific. Mar Ecol Prog Ser 387:1–14

Fang Z, Xu L, Chen X, Liu B, Li J, Chen Y (2015) Beak growth pattern of purpleback flying squid *Sthenoteuthis oualaniensis* in the eastern tropical Pacific equatorial waters. Fish Sci 81:443–452

Fernández-Álvarez FÁ, Martins CPP, Vidal EAG, Villanueva R (2017) Towards the identification of the ommastrephid squid paralarvae (Mollusca: Cephalopoda): morphological description of three species and a key to the north-east Atlantic species. Zool J Linn Soc 180:268–287

Fernández-Álvarez FÁ, Machordom A, García-Jiménez R, Salinas-Zavala CA, Villanueva R (2018) Predatory flying squids are detritivores during their early planktonic life. Sci Rep 8:3440

Field JC, Elliger C, Baltz K, Gillespie GE and others (2013) Foraging ecology and movement patterns of jumbo squid (*Dosidicus gigas*) in the California Current System. Deep Sea Res II 95:37–51

Folmer O, Hoeh WR, Black MB, Vrijenhoek RC (1994) Conserved primers for PCR amplification of mitochondrial DNA from different invertebrate phyla. Mol Mar Biol Biotechnol 3:294–299

Franco-Santos RM, Vidal EAG (2014) Beak development of early squid paralarvae (Cephalopoda: Teuthoidea) may reflect an adaptation to a specialized feeding mode. Hydrobiologia 725:85–103

Frézal L, Leblois R (2008) Four years of DNA barcoding: current advances and prospects. Infect Genet Evol 8: 727–736

Friedemann K, Wolff M, Argüelles J, Mariátegui L, Tafur R, Yamashiro C (2008) A hypothesis on range expansion and spatio-temporal shifts in size-at-maturity of jumbo squid (*Dosidicus gigas*) in the eastern Pacific Ocean. CCOFI Rep 49:119–128

Galván DE, Sweeting CJ, Reid WDK (2010) Power of stable isotope techniques to detect size-based feeding in marine fishes. Mar Ecol Prog Ser 407:271–278

Gilly WF, Markaida U, Baxter CH, Block BA and others (2006) Vertical and horizontal migrations by the jumbo squid *Dosidicus gigas* revealed by electronic tagging. Mar Ecol Prog Ser 324:1–17

Gong Y, Li Y, Chen X, Chen L (2018a) Potential use of stable isotope and fatty acid analyses for traceability of geographic origins of jumbo squid (*Dosidicus gigas*). Rapid Commun Mass Spectrom 32:583–589

Gong Y, Ruiz-Cooley RI, Hunsicker ME, Li Y, Chen X

(2018b) Sexual dimorphism in feeding apparatus and niche partitioning in juvenile jumbo squid *Dosidicus gigas*. Mar Ecol Prog Ser 607:99–112

Gong Y, Li Y, Chen X, Yu W (2020) Trophic niche and diversity of a pelagic squid (*Dosidicus gigas*): a comparative study using stable isotope, fatty acid, and feeding apparatuses morphology. Front Mar Sci 7:642

Henderson RJ, Sargent JR, Hopkins CCE (1984) Changes in the content and fatty acid composition of lipid in an isolated population of the capelin *Mallotus villosus* during sexual maturation and spawning. Mar Biol 78:255–263

Hourston M, Platell ME, Valesini FJ, Potter IC (2004) Factors influencing the diets of four morphologically divergent fish species in nearshore marine waters. J Mar Biol Assoc UK 84:805–817

Hyslop EJ (1980) Stomach contents analysis — a review of methods and their application. J Fish Biol 17:411–429

Ibáñez CM, Arancibia H, Cubillos LA (2008) Biases in determining the diet of jumbo squid *Dosidicus gigas* (D' Orbigny 1835) (Cephalopoda: Ommastrephidae) off southern-central Chile (34°S–40°S). Helgol Mar Res 62: 331–338

Iverson SJ, Field C, Bowen WD, Blanchard W (2004) Quantitative fatty acid signature analysis: a new method of estimating predator diets. Ecol Monogr 74:211–235

Jackson AL, Inger R, Parnell AC, Bearhop S (2011) Comparing isotopic niche widths among and within communities: SIBER — stable isotope Bayesian ellipses in R. J Anim Ecol 80:595–602

Jones JB, Pierce GJ, Saborido-Rey F, Brickle P, Kuepper FC, Shcherbich ZN, Arkhipkin AI (2019) Size-dependent change in body shape and its possible ecological role in the Patagonian squid (*Doryteuthis gahi*) in the southwest Atlantic. Mar Biol 166:1–17

Kelly JR, Scheibling RE (2012) Fatty acids as dietary tracers in benthic food webs. Mar Ecol Prog Ser 446:1–22

Kharlamenko VI, Kiyashko SI, Imbs AB, Vyshkvartzev DI (2001) Identification of food sources of invertebrates from the seagrass *Zostera marina* community using carbon and sulfur stable isotope ratio and fatty acid analyses. Mar Ecol Prog Ser 220:103–117

Kier WM, Smith KK (1985) Tongues, tentacles and trunks: the biomechanics of movement in muscular-hydrostats. Zool J Linn Soc 83:307–324

Kováč V, Copp GH, Francis MP (1999) Morphometry of the stone loach, *Barbatula barbatula*: Do mensural characters reflect the species' life history thresholds? Environ Biol Fishes 56:105–115

Leray M, Yang JY, Meyer CP, Mills SC and others (2013) A new versatile primer set targeting a short fragment of the mitochondrial COI region for metabarcoding metazoan diversity: application for characterizing coral reef fish gut contents. Front Zool 10:34

Li Y, Gong Y, Zhang Y, Chen X (2017) Inter-annual variability in trophic patterns of jumbo squid (*Dosidicus gigas*) off the exclusive economic zone of Peru, implications from stable isotope values in gladius. Fish Res 187:22–30

Liu B, Chen X, Fang Z (2017) Statolith microstructure, age, and maturity of jumbo squid (*Dosidicus gigas*) in equatorial waters of the eastern tropical Pacific Ocean. Bull Mar Sci 93:943–957

Liu BL, Xu W, Chen XJ, Huan MY, Liu N (2020) Ontogenetic shifts in trophic geography of jumbo squid, *Dosidicus gigas*, inferred from stable isotopes in eye lens. Fish Res 226:105507

Lorrain A, Argüelles J, Alegre A, Bertrand A, Munaron JM, Richard P, Cherel Y (2011) Sequential isotopic signature along gladius highlights contrasted individual foraging strategies of jumbo squid (*Dosidicus gigas*). PLOS ONE 6:e22194

Lundvall D, Svanbäck R, Persson L, Byström P (1999) Size-dependent predation in piscivores: interactions between predator foraging and prey avoidance abilities. Can J Fish Aquat Sci 56:1285–1292

MacArthur RH, Pianka ER (1966) On optimal use of a patchy environment. Am Nat 100:603–609

Markaida U, Sosa-Nishizaki O (2003) Food and feeding habits of jumbo squid *Dosidicus gigas* (Cephalopoda: Ommastrephidae) from the Gulf of California, Mexico. J Mar Biol Assoc UK 83:507–522

Miller TW, Bosley KL, Shibata J, Brodeur RD, Omori K, Emmett R (2013) Contribution of prey to Humboldt squid *Dosidicus gigas* in the northern California Current, revealed by stable isotope analyses. Mar Ecol Prog Ser 477:123–134

Narváez M, Freites L, Guevara M, Mendoza J, Guderley H, Lodeiros CJ, Salazar G (2008) Food availability and reproduction affects lipid and fatty acid composition of the brown mussel, *Perna perna*, raised in suspension culture. Comp Biochem Physiol B Biochem Mol Biol 149: 293–302

Nesis K (1970) The biology of the giant squid of Peru and Chile, *Dosidicus gigas*. Oceanology (Mosc) 10:108–118

Nigmatullin CM, Nesis KN, Arkhipkin AI (2001) A review of the biology of the jumbo squid *Dosidicus gigas* (Cephalopoda: Ommastrephidae). Fish Res 54:9–19

Nödl MT, Kerbl A, Walzl MG, Müller GB, de Couet HG (2016) The cephalopod arm crown: appendage formation and differentiation in the Hawaiian bobtail squid *Euprymna scolopes*. Front Zool 13:44

Nogueira N, Fernandes I, Fernandes T, Cordeiro N (2017) A comparative analysis of lipid content and fatty acid composition in muscle, liver and gonads of *Seriola fasciata* Bloch 1793 based on gender and maturation stage. J Food Compos Anal 59:68–73

Pethybridge HR, Choy CA, Polovina JJ, Fulton EA (2018) Improving marine ecosystem models with biochemical tracers. Annu Rev Mar Sci 10:199–228

Portner EJ, Markaida U, Robinson CJ, Gilly WF (2020) Trophic ecology of Humboldt squid, *Dosidicus gigas*, in conjunction with body size and climatic variability in the Gulf of California, Mexico. Limnol Oceanogr 65:732–748

Post DM (2002) Using stable isotopes to estimate trophic position: models, methods, and assumptions. Ecology 83: 703–718

R Core Team (2019) R: a language and environment for statistical computing. R Foundation for Statistical Computing, Vienna

Rodhouse PG, Nigmatullin CM (1996) Role as consumers. Philos Trans R Soc B 351:1003–1022

Rosa R, Seibel BA (2010) Metabolic physiology of the Humboldt squid, *Dosidicus gigas*: implications for vertical migration in a pronounced oxygen minimum zone. Prog Oceanogr 86:72–80

Rosas-Luis R, Tafur-Jimenez R, Alegre-Norza AR, Castillo-Valderrama PR, Cornejo-Urbina RM, Salinas-Zavala CA, Sánchez P (2011) Trophic relationships between the jumbo squid (*Dosidicus gigas*) and the lightfish (*Vinciguerria lucetia*) in the Humboldt Current System off Peru. Sci Mar 75:549–557

Ruiz-Cooley RI, Markaida U, Gendron D, Aguíñiga S (2006) Stable isotopes in jumbo squid (*Dosidicus gigas*) beaks to estimate its trophic position: comparison between stomach contents and stable isotopes. J Mar Biol Assoc UK 86: 437–445

Saito H, Murata M (1998) Origin of the monoene fats in the lipid of midwater fishes: relationship between the lipids of myctophids and those of their prey. Mar Ecol Prog Ser 168:21–33

Saito H, Sakai M, Wakabayashi T (2014) Characteristics of the lipid and fatty acid compositions of the Humboldt squid, *Dosidicus gigas*: the trophic relationship between the squid and its prey. Eur J Lipid Sci Technol 116: 360–366

Sardenne F, Bodin N, Chassot E, Amiel A and others (2016) Trophic niches of sympatric tropical tuna in the western Indian Ocean inferred by stable isotopes and neutral fatty acids. Prog Oceanogr 146:75–88

Scharf FS, Juanes F, Rountree RA (2000) Predator size–prey size relationships of marine fish predators: interspecific variation and effects of ontogeny and body size on trophic-niche breadth. Mar Ecol Prog Ser 208:229–248

Shea EK (2005) Ontogeny of the fused tentacles in three species of ommastrephid squids (Cephalopoda, Ommastrephidae). Invertebr Biol 124:25–38

Shetinnikov A (1989) Food spectrum of the squid *Dosidicus gigas* (Oegopsida) in the ontogenesis. Zool Zh 68:28–39

Shigeno S, Kidokoro H, Goto T, Tsuchiya K, Segawa S (2001) Early ontogeny of the Japanese common squid *Todarodes pacificus* (Cephalopoda, Ommastrephidae) with special reference to its characteristic morphology and ecological significance. Zool Sci 18:1011–1026

Skieresz-Szewczyk K, Jackowiak H (2016) Morphofunctional study of the tongue in the domestic duck (*Anas platyrhynchos f. domestica*, Anatidae): LM and SEM study. Zoomorphology 135:255–268

Stewart JS, Field JC, Markaida U, Gilly WF (2013) Behavioral ecology of jumbo squid (*Dosidicus gigas*) in relation to oxygen minimum zones. Deep Sea Res II 95:197–208

Teuber L, Schukat A, Hagen W, Auel H (2014) Trophic interactions and life strategies of epi- to bathypelagic calanoid copepods in the tropical Atlantic Ocean. J Plankton Res 36:1109–1123

Trasviña-Carrillo LD, Hernández-Herrera A, Torres-Rojas YE, Galván-Magaña F, Sánchez-González A, Aguíñiga-García S (2018) Spatial and trophic preferences of jumbo squid *Dosidicus gigas* (D'Orbigny, 1835) in the central Gulf of California: ecological inferences using stable isotopes. Rapid Commun Mass Spectrom 32:1225–1236

Vasconcellos RM, Gomes-Gonçalves RS, Santos JNS, Cruz Filho AG, Araújo FG (2018) Do closely related species share of feeding niche along growth? Diets of three sympatric species of the mojarras (Actinopterygii: Gerreidae) in a tropical bay in southeastern Brazil. Environ Biol Fishes 101:949–962

Ventura D, Bonhomme V, Colangelo P, Bonifazi A, Jona Lasinio G, Ardizzone G (2017) Does morphology predict trophic niche differentiation? Relationship between feeding habits and body shape in four co-occurring juvenile species (Pisces: Perciformes, Sparidae). Estuar Coast Shelf Sci 191:84–95

Volkman JK, Jeffrey SW, Nichols PD, Rogers GI, Garland CD (1989) Fatty acid and lipid composition of 10 species of microalgae used in mariculture. J Exp Mar Biol Ecol 128:219–240

Werner EE, Gilliam JF (1984) The ontogenetic niche and species interactions in size-structured populations. Annu Rev Ecol Syst 15:393–425

Xu W, Chen X, Liu B, Chen Y, Huan M, Liu N, Lin J (2019) Inter-individual variation in trophic history of *Dosidicus gigas*, as indicated by stable isotopes in eye lenses. Aquacult Fish 4:261–267

Young T, Pincin J, Neubauer P, Ortega-García S, Jensen OP (2018) Investigating diet patterns of highly mobile marine predators using stomach contents, stable isotope, and fatty acid analyses. ICES J Mar Sci 75:1583–1590

Editorial responsibility: Stephen Wing, Dunedin, New Zealand
Reviewed by Y. Kawabata and 2 anonymous referees

Submitted: August 22, 2021
Accepted: May 10, 2022
Proofs received from author(s): June 27, 2022